NOAA Technical Report ERL 419-PMEL 36

A Climatology of the Bering Sea and Its Relation to Sea Ice Extent

Carol H. Pease
Sally A. Schoenberg
James E. Overland

Pacific Marine Environmental Laboratory
Seattle, Washington

March 1982

U.S. Department of Commerce
Malcolm Baldrige, Secretary

National Oceanic and Atmospheric Administration
John V. Byrne, Administrator

Environmental Research Laboratories
Boulder, Colorado
George H. Ludwig, Director

NOTICE

Mention of a commercial company or product does not constitute an endorsement by NOAA Environmental Research Laboratories. Use for publicity or advertising purposes of information from this publication concerning proprietary products or the tests of such products is not authorized.

CONTENTS

A Climatology of the Bering Sea and Its Relation to Sea Ice Extent

Carol H. Pease, Sally A. Schoenberg, James E. Overland

ABSTRACT. The relation between interannual variations in maximum sea ice extent and atmospheric forcing within the region of the Bering Sea is discussed. Monthly maximum sea ice extents for February and March along a line from Norton Sound southwest toward the ice edge are computed for the ice years 1955/56 to 1979/80 and analyzed for each month's average and each year's seasonal maximum ice extent. A storm track climatology is developed by computing monthly cyclone frequencies for each 2°-latitude by 4°-longitude quadrangle within 51°N-65°N, 157°W-171°E from November 1957 through March 1980. Five-day block-averaged sea level pressure fields are analyzed from 1954/55 through 1976/77 by month and year for mean sea level pressure and pressure variance climatologies. The annual winter cycle of the storm count maxima, mean pressure minima, and variance maxima resemble each other closely. The interannual variability of maximum sea ice extent is related to the storm track, mean sea level pressure, and pressure variance climatologies, indicating that in years of greatest ice extent, fewer storms enter the region, and low-pressure centers are quasi-stationary in the western Gulf of Alaska and southeastern Bering Sea. Years of least ice extent are characterized by more storms penetrating the region, particularly in the western sector, and by a larger variance in atmospheric pressure everywhere. Meteorological steering of cyclones, determined primarily externally to the Bering Sea, is indicated as the principal factor causing the interannual variability of sea ice extent.

1. INTRODUCTION

In this century the Bering Sea has been completely ice free in summer, but ice covered over much of the extensive continental shelf region in winter. In October and November, ice forms in situ along the coasts in the northern part of the Bering Sea basin. Predominantly northeasterly winds drive this ice toward the southwest creating polynyas along the southern side of Seward Peninsula and St. Lawrence Island (fig. 1). These coastal polynyas act as production sites for new ice during most of the winter (Fay, 1974; Muench and Ahlnäs, 1976; McNutt, 1981a,b). The leading floes along the edge of the pack ice are advected into water that is warmer than the freezing point, and the floes melt. The addition of melt water and the large, sensible heat flux from the ocean to the cold, off-ice winds cool the ocean so that the pack extent may advance (Pease, 1980). Thus, in midwinter, movement characteristics of the ice can be described as a kind of conveyor belt: ice grows primarily in the north, is advected by wind stress generally southward, and decays at the southern thermodynamic limit. The ice may replace itself two to five times during a winter season by this mechanism, which represents a substantial

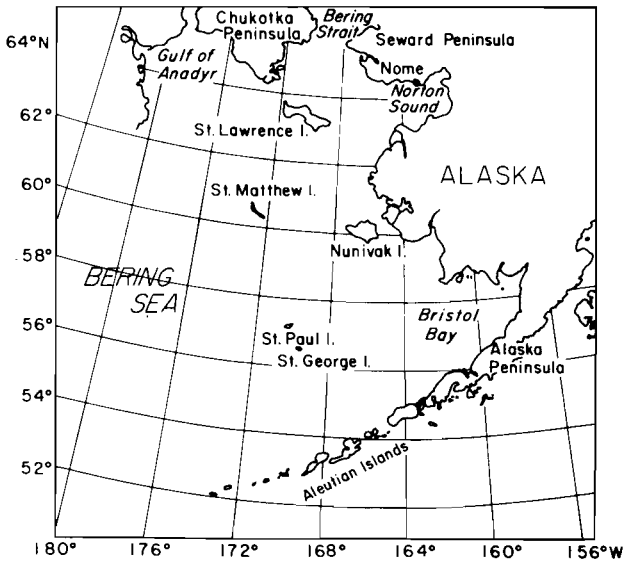

Figure 1.--The eastern Bering Sea region.

latitudinal heat flux (Pease, 1980). Advection of sea ice by currents is of secondary importance south of St. Lawrence Island since tidal currents dominate the horizontal kinetic energy on the continental shelf and vector mean flow is 1-5 cm s^{-1} toward the north or northwest (Kinder and Schumacher, 1981b). In a year of large ice extent ("heavy ice year"), the pack will reach St. Paul Island and beyond; whereas in a year of small ice extent ("light ice year"), the pack may reach only beyond St. Matthew and Nunivak Islands (Webster, 1979). Yearly maximum extent typically occurs between mid-February and late March (Dunbar, 1967). At approximately the time of the vernal equinox, the radiation balance at the surface of the ice changes so that the ice melts over most of the basin even under continued northeasterly winds. Increased south-to-southeasterly winds also contribute to spring decay. Sea ice is absent by the end of June.

Although many of the individual features of the dynamics and thermodynamics of Bering Sea ice have been explored and the seasonal cycle explained (Niebauer, 1980), the nature of the relation between interannual variations in sea ice extent and atmospheric forcing has not been discussed in detail except as part of a larger study of the Arctic by Johnson (1980). Rapid ice advance is thought to occur with northeasterly winds when Arctic high pressure dominates the northern Bering Sea and eastern Siberia. Cyclones passing over the region interrupt these northeasterly winds and can even cause the ice edge to retreat. Hence, the frequency of cyclones should be an important factor in determining the overall maximum ice extent in any given year.

Further research on short-term and interannual variations in sea ice conditions around Alaska is motivated by several different issues. Recent expansion of the Bering Sea fisheries to year-round operation, the impending development of offshore energy resources, and the increase of shipping through the Bering and Chukchi seas for the activities of the petroleum industry on the North Slope have emphasized the requirement for more accurate forecasts of pack ice location, condition, and movement. Accurate analyses and forecasts are essential to minimize the loss of lives, vessels, and equipment and to improve efficiency of operations for various industries affected by ice.

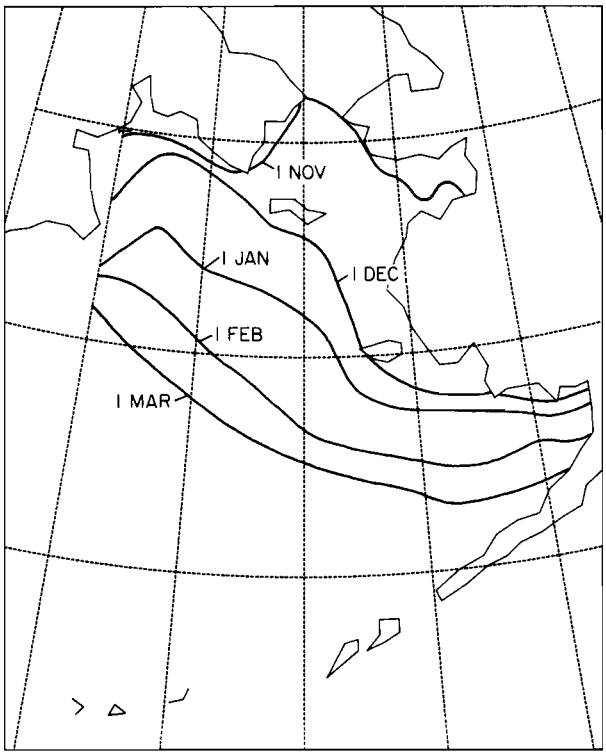

Figure 2.--Average progression (50% probability) of ice extent during the growth season, based on 1972-1979 ice extents (adapted from Webster, 1979).

2. SEA ICE CLIMATOLOGY

2.1 Annual Cycle

Ice typically starts forming in October in the eastern reaches of Norton Sound, in the slightly brackish waters of the Yukon River Delta, and in the Gulf of Anadyr (Webster, 1979). On the average, a period of substantial advance of ice extent occurs between 1 November and 1 December (fig. 2). This advance is typically 2°-3° latitude (200-300 km) and is accomplished by in situ growth shifting to the conveyor belt process. No surface observations of the transition from one regime to the other have been made, since the period is fairly hazardous for direct observations because of light limitations and relatively thin ice conditions. However, ARGOS (satellite) buoys deployed in the Nome area in January 1981 drifted toward the southwest with the conveyor drift pattern (D. Thomas; Flow Research, Kent, Wash.; personal communication, 1981), and many satellite observations confirming drift have been made between February and June of various years (McNutt, 1981a,b; Muench and Ahlnäs, 1976).

In succeeding months, through March, the ice edge advances at a rate averaging 150-200 km mo^{-1} (fig. 2). This progression is not entirely steady, however. With each cyclone that penetrates the region there is a temporary retreat, so the advance is a two-steps-forward, one-step-back process. Since wind stress transmitted to the ice is proportional to the square of the velocity, one cyclone penetrating the region for a few days can undo the work of relatively weak northeastern winds of almost a week, as was observed in 1981 (Pease and Muench, 1981). Spring decay occurs throughout the pack at about the same rate everywhere, but thicker ice may be advected around the

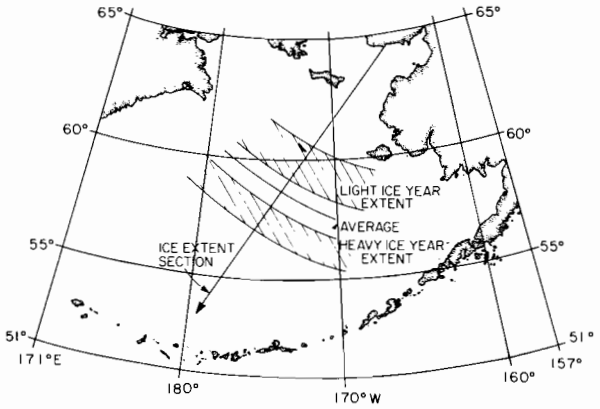

Figure 3.--Section along which maximum winter ice extents were computed, and the range of the five lightest and five heaviest extents during 1956-1980 relative to the section.

basin until late June. After March and April, new ice is not formed under continued northeasterly winds, so the polynyas remain open and increase in size.

2.2 Interannual Variations

The ice extent data available for the Bering Sea varies widely in quality and quantity between the early 1950's and the present. Satellite observations of the ice extent are available for 1967 through the present. Prior to 1967, ice extent was recorded by direct observation from ships or through occasional ice reconnaissance flights by the Navy and others. Most of the available observations of hemispheric ice extent and concentration from 1952 to 1977 have been collected by Walsh and Johnson (1979a,b) and blocked into 1°-latitude-equivalent areas by month. Walsh and Johnson included average monthly ice concentration over all years for any given area when no observations were available during a given month. Unfortunately, they were particularly forced to use this method west of 180°W and in Bristol Bay in the Bering Sea. Therefore, to avoid biasing the ice extent estimates by their averaging procedure, ice extent was calculated for this study using the Walsh-Johnson data set for winters 1955/56 to 1970/71 along a section of their grid in the eastern Bering Sea, shown in fig. 3. This section is located approximately along the climatological ice floe trajectory path, from Norton Sound southwest to the ice edge. For winters 1971/72 to 1979/80, ice extents have been computed from monthly averages of the U.S. Navy-NOAA Joint Ice Center charts. All years have been compared with available naval air reconnaissance data.

Table 1 lists the ice extents along the track shown in fig. 3 for February and March and indicates the five heaviest (1957/58, 1960/61, 1963/64, 1975/76, 1976/77) and five lightest (1958/59, 1965/66, 1966/67, 1977/78, 1978/79) ice years in the record. The range of the five heaviest and five lightest ice years is also plotted in fig. 3. These maximum and minimum years differ from those of Walsh and Johnson (1979b) because they used January values for their maximum extents over the Arctic Basin. January values, however, are not representative of the overall winter signal for the Bering Sea. There exists a tendency for maximum extent to occur in February in heavy ice years and in March otherwise. Of the five winters identified in table 1

Table 1.--Average February and March ice extent in the Bering Sea along the section shown in fig. 3

Year	February extent (km)[1]	March extent (km)[1]	Confidence[2] in extent (km)	Heavy (H) or light (L) ice
1956	670	800	±100	(L)[3]
1957	770	870	"	
1958	930	660	"	H
1959	550	670	"	L
1960	700	800	"	
1961	960	970	"	H
1962[4]	760	770	±200	
1963	770	810	±100	
1964	1030[5]	930	"	H
1965	800	800	"	
1966	465	540	"	L
1967	660	430	"	L
1968	860	720	"	
1969	670	770	±50	(L)[3]
1970	690	800	"	
1971	870	870	"	
1972[6]	780	890	"	
1973	680	870	"	
1974	800	790	"	
1975	770	790	"	
1976	940	910	"	H
1977	890	830	"	H
1978	670	750	"	L
1979	560	650	"	L
1980	750	780	"	

[1] February average extent $\bar{x}$ = 759.8 km, S.D. = 137.9; March average extent $\bar{x}$ = 778.8 km, S.D. = 122.5. Maximum, either month: $\bar{x}$ = 814.2 km, S.D. = 110.1.

[2] Subjective assessment based on frequency and coverage of the Bering Sea by U.S. Navy ice reconnaissance flights prior to 1969 and thereafter on the resolution and cloud-free coverage by NOAA satellite visual and infrared imagery.

[3] Alternate light ice years to substitute for 1978 and 1979 for the pressure analysis because of incomplete modern pressure fields for those years.

[4] No U.S. Navy ice reconnaissance missions were flown in the western Arctic in 1962, so average February and March values are used. Note that this is not the same as the mean maximum extent. See footnote 1.

[5] Revised downward from Walsh and Johnson (1979a) data. New value is consonant with U.S. Navy ice reconnaissance observations during the winter of 1964.

[6] Values for 1972-1980 were obtained by averaging weekly ice extents from analysis maps from the U.S. Navy-NOAA Joint Ice Center in Suitland, Maryland.

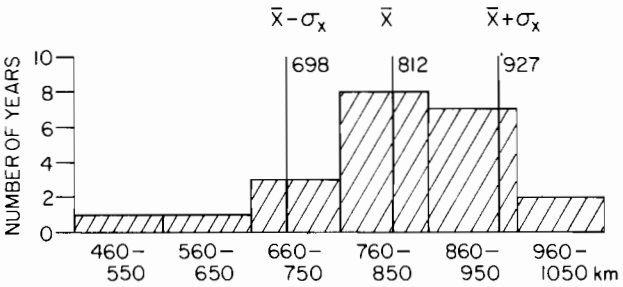

Figure 4.--Distribution of maximum ice extents, 1956-1980.

as heavy ice years, four have their maximum ice extent in February; of the five winters identified as light ice years, four have their maximum in March. In fact, only 7 of 25 years have maximum extent in February. The variance of the ice extent along the trackline is 28% greater in February than in March. March is the great equalizer: heavy ice extent in February tends to decline in March, and light ice extent in February tends to increase in March, although there is an overall bias for a maximum in March. The standard deviation of the maximum extent is less than the standard deviation in either month.

The distribution of maximum ice extent by 100-km class intervals in fig. 4 is skewed toward heavy ice years. This may be evidence that there is some constraint on extremely heavy maximum ice extents. Possible constraint mechanisms are (1) the change in radiation balance at more southerly latitudes as the equinox approaches, (2) increased influence of the northwestward-flowing slope current along the shelf break in the Bering Sea (Kinder and Schumacher, 1981b), or (3) the inability of melting ice to cool the mixed layer to the freezing point beyond the outer continental shelf (Kinder and Schumacher, 1981a). The latter mechanism seems to be the most important consideration in recent winters (Pease and Muench, 1981).

3. RELATION OF SEA ICE TO ATMOSPHERIC VARIABILITY

3.1 Background

Studies beginning early this century have indicated relationships between sea ice extent and anomalies in certain atmospheric fields such as sea level pressure, air temperature, and precipitation. It is known that ice growth depends upon such atmospheric parameters as air temperature, wind velocity, and cloud cover, and that ice transport depends upon wind and current velocities. On the other hand, sea ice extent and its snow cover modify the surface albedo and drastically reduce the sensible and latent heat flux to the atmosphere from subpolar oceans. The presence of an ice edge produces large horizontal gradients in these fluxes.

Empirical studies of ice extent and atmospheric circulation can be divided into those of regional scale (Wiese, 1924; Walker and Bliss, 1932;

Schell, 1964; Crane, 1978; Rogers, 1981) and those of hemispheric scale (Schwerdtferger and Kachelhoffer, 1973; Walsh and Johnson, 1979b). In the Northern Hemisphere, study of the large-scale situation is made complex by the coexistence of sea ice zones and land masses along a given latitude circle. Any interannual variability in sea ice extent will force the atmosphere only in very specific locations. Also, the problem of feedback between ice and the atmosphere is complicated by the different kinds of sea ice forcing that are active in different parts of the hemisphere. Ice in the East Greenland Sea is strongly influenced by ocean currents (Wadhams, 1981). Rogers (1978) has shown that the number of thawing degree days is the parameter most highly correlated with location of the summertime ice margin in the Beaufort Sea. Thus, there exists a need to investigate regional interaction to aid understanding of hemispheric-scale questions in addition to the more direct application of local ice edge forecasting.

3.2 Regional Surface Observations

The first accurate description of the regional ice dynamics in the Bering Sea was given by biologist Fay (1974). From his experiences on the ice while studying marine mammals, Fay surmised that ice floes were formed in the northern Bering Sea and drifted toward the southwest under the influence of predominantly northeasterly winds derived from the Arctic high- and Aleutian low-pressure systems. Further, he described the influence of the occasional penetration of low-pressure centers over the southern pack ice. These lows cause the temporary northward advection of sea ice by southerly winds and the mechanical breaking of the retreating ice floes by swell.

Observations of ice drift were made during the Bering Sea Experiment (BESEX) from the USCG cutter *Staten Island* from 16 February to 6 March 1973 by allowing the ship to drift with the pack at night (Campbell et al., 1974). Although these observations were biased by the ship's sail area, the ice was observed to drift principally south to southwest with a reversal in drift during the passage of a low-pressure center. Ship drift speeds ranged from 0.25 to 0.50 m s^{-1} from a variety of locations. These were about 0.02-0.03 times the windspeed.

Using satellite imagery for the spring of 1974, Muench and Ahlnäs (1976) verified the ice drift out of Norton Sound and the northern Bering Sea and gave quantitative estimates of floe velocity averaging 0.25 m s^{-1} and ranging to 0.50 m s^{-1}. Similar floe speed ranges were observed by McNutt (1981a,b) using additional satellite photograph analysis for other winters during periods of northerly winds. These studies were limited by their dependence on visual satellite photography. Although good estimates of southward drift were obtained, periods of suspected northward drift were obscured by clouds, and little information was available for the area along the ice edge or on meteorological parameters.

Surface field observations were carried out along the ice edge from the NOAA ship *Surveyor* in March 1979. Observations from the ship included radiosonde measurements of potential temperature in the atmospheric boundary layer, which indicated both growth of the boundary layer height and increase in the surface air temperature with distance away from the ice, during off-ice winds

(Salo et al., 1980). Under certain temperature and wind conditions this convection became organized into regular horizontal roll vortices, which are closely aligned to the direction of the wind, and roll clouds formed (Walter, 1980). These vortices persisted for several hundred kilometers south of the ice edge.

A second cruise to the ice edge by the *Surveyor* in February and March 1981 was planned to track individual floes near the ice edge. However, the first week of operations was interrupted by the passage of a 956-mb low-pressure center with accompanying southerly winds of 15-20 m s^{-1} and 5-m swell. This gale drove the ice toward the north for more than 100 km in 3 days and mechanically ground the ice in the vicinity of the ice edge from floe diameters of 10-50 m before the storm to 1-5 m after the storm (Pease and Muench, 1981). After the passage of the storm the wind shifted back to northeasterly, and floe drift resumed toward the southwest. It took almost a week for the ice edge to regain its original position (Pease and Muench, 1981). Floe drift velocities measured with ARGOS ice buoys indicated that southward floe velocities after the storm were similar to those observed from satellite photograph analyses for the northern Bering, but during the storm the northward velocities were two or three times the previous measurements.

3.3 Approach to the Problem

Three basic approaches have been used to generalize the synoptic variability in a given region: a synoptic climatology (Barry and Perry, 1973), which regards patterns of weather as implicit functions of the sea level pressure distribution; a kinematic approach, in which synoptic weather maps are classified in terms of principal storm tracks; and a variance of sea level pressure, which is preferred for hemispheric studies (Walker and Bliss, 1932; Blackmon et al., 1977; Rogers, 1981). A synoptic climatology is most appropriate where a portion of the sea level pressure features form or decay in situ or are particularly persistent (Suckling and Hay, 1978; Overland and Hiester, 1980). A synoptic climatology was used for the study of sea ice extent for Davis Strait by Crane (1978). The two synoptic climatologies covering the northern Bering Sea (Putnins, 1966; Barry, 1977) indicate a major first weather type associated with Arctic high pressure. The remaining weather types, however, tend to have nearly the same frequency of occurrence and appear to be arbitrary in location, indicating that there is not a strong locational preference for synoptic features.

Previous analyses of both cyclone and anticyclone frequency patterns have included the Bering Sea only as part of studies of larger areas--as in the hemispheric studies of Petterssen (1956) and Klein (1957). Klein used a grid of 5° latitude by 5° longitude to determine the spatial distribution of cyclone and anticyclone frequencies for individual months using the daily synoptic series for 1899-1939. He constructed principal tracks drawn through axes of maximum frequency that corresponded to the major trough along the Aleutian Islands into the Gulf of Alaska. Blasing and Fritts (1976) determined a synoptic climatology based upon sea level pressure for December through February and produced cyclone charts for each weather type. Over the Bering Sea, their two major types showed a northwest-southeast shift in storm tracks.

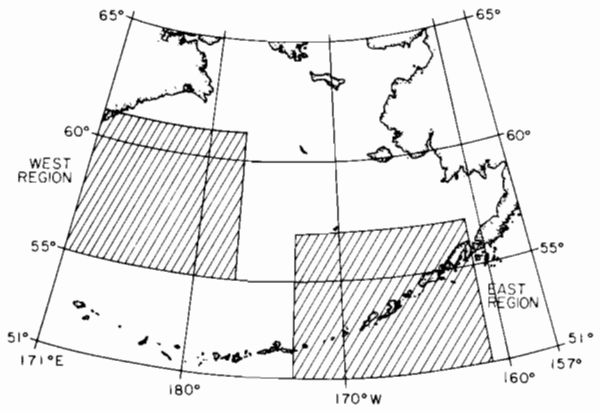

Figure 5.--Regions of cyclone counts for cyclone index 1 (the number of storms, October-February, in the Eastern sector minus the number in the Western sector).

4. CYCLONE CLIMATOLOGY

4.1 Methods

The data used in this study were derived from monthly maps of cyclone tracks published in the *Mariners Weather Log* for November 1957 through March 1980. Locations for pressure centers are given on these charts for 00 and 12 GMT. Storm (cyclone) tracks for October 1957 were computed directly from daily sea level pressure charts to complete the ice year for winter 1957/58. To study horizontal distributions, 2°-latitude by 4°-longitude grids were prepared, and cyclone frequencies were determined by counting the number of cyclone tracks that passed through each quadrangle in a particular month and year. Although the area enclosed by the quadrangles decreases with increasing latitude, no areal corrections were made (Zishka and Smith, 1980; Hayden, 1981). Quadrangles of this size were used because using smaller areas qualitatively resulted in noisy fields.

Linear indices of storm patterns were developed by summing the number of storm centers within subregions of the Bering Sea. Index 1 is the number of storms for each ice growth season, October through February, in the eastern sector (fig. 5) minus the number in the western sector. These sectors were chosen to enclose the regions that had a maximum variance in number of storms. This index differentiates between east and west dominance of storm tracks. Index 2 is the number of storms in a given ice season that reach north of 59°N; i.e., it is an index of the total number of storms penetrating the Bering Sea marginal ice zone. Index 3 is the amplitude of the first empirical orthogonal function (EOF) of storm track spatial correlation for October through February (Overland and Preisendorfer, 1982).

The first EOF resolves 22.3% of the variance of the 23-yr normalized storm track maps; only the first EOF pattern is statistically significant in terms of the Rule N test (Preisendorfer and Barnett, 1977; Overland and Preisendorfer, 1982). These two features of the EOF analysis can be interpreted as an indication that the 2°-latitude by 4°-longitude sums for an individual year are still noisy, whereas means over larger areas, as in index 1, or monthly means over 23 years add to the stability of the estimates.

To investigate the relation between storm tracks and sea ice extent for heavy, light, and average ice conditions, storms from October through February (5 months) for each year and for each square in the storm track grid were summed. Then storms in the five heavy years and the five light years, given in table 1, were individually summed. In addition, storms in all 23 years in the meteorological record were summed, and these numbers were scaled by dividing the sums by 23, and multiplied by 5, to estimate a regional mean pattern for comparison with the light and heavy groupings.

4.2 Annual Cycle

Figure 6 shows the number of storms passing through each quadrangle for the 23-yr period from 1957 to 1979 for October through December, and from 1958 to 1980 for January through March. October shows a tendency for two tracks, one starting in the lower left corner at 179°E, 51°N and heading east-northeast parallel to the Aleutian Islands. The other track enters at 171°E, 56°N and curves northward toward Bering Strait and the Chukotka Peninsula. This northerly track is not as evident in following months because the dominant Siberian high pressure is established in the northwest corner of the region. November has a maximum at 170°W, 55°N with an indication of two tracks passing through this region: one parallel to the Aleutians as in October, and one curving north into the Bering along 170°W. This northerly track persists through February; however, the absolute frequency of storms drops substantially with latitude in all months. The relative importance of the northern track peaks in January when the frequency along this track is of a magnitude similar to that of the southerly track along the eastern part of the Aleutians. This month corresponds to maximum blocking-ridge activity in the North Pacific as given by White and Clark (1975). They show that 29% of the 31 Januarys from 1959 to 1970 had blocking-ridge activity as compared with 10% for the months of December and February. In March the overall storm activity increases, and the frequencies at all latitudes have a more zonal character than in midwinter.

Figure 7 shows the zonal average frequency between 160°W and 180°W as a function of month, illustrating the latitudinal dependence of the annual signal. These figures have been normalized by month and by area. There is an annual signal with an overall minimum in January and February. The latitudinal gradient of storms is roughly constant for all months except January, which has a more uniform north-south gradient.

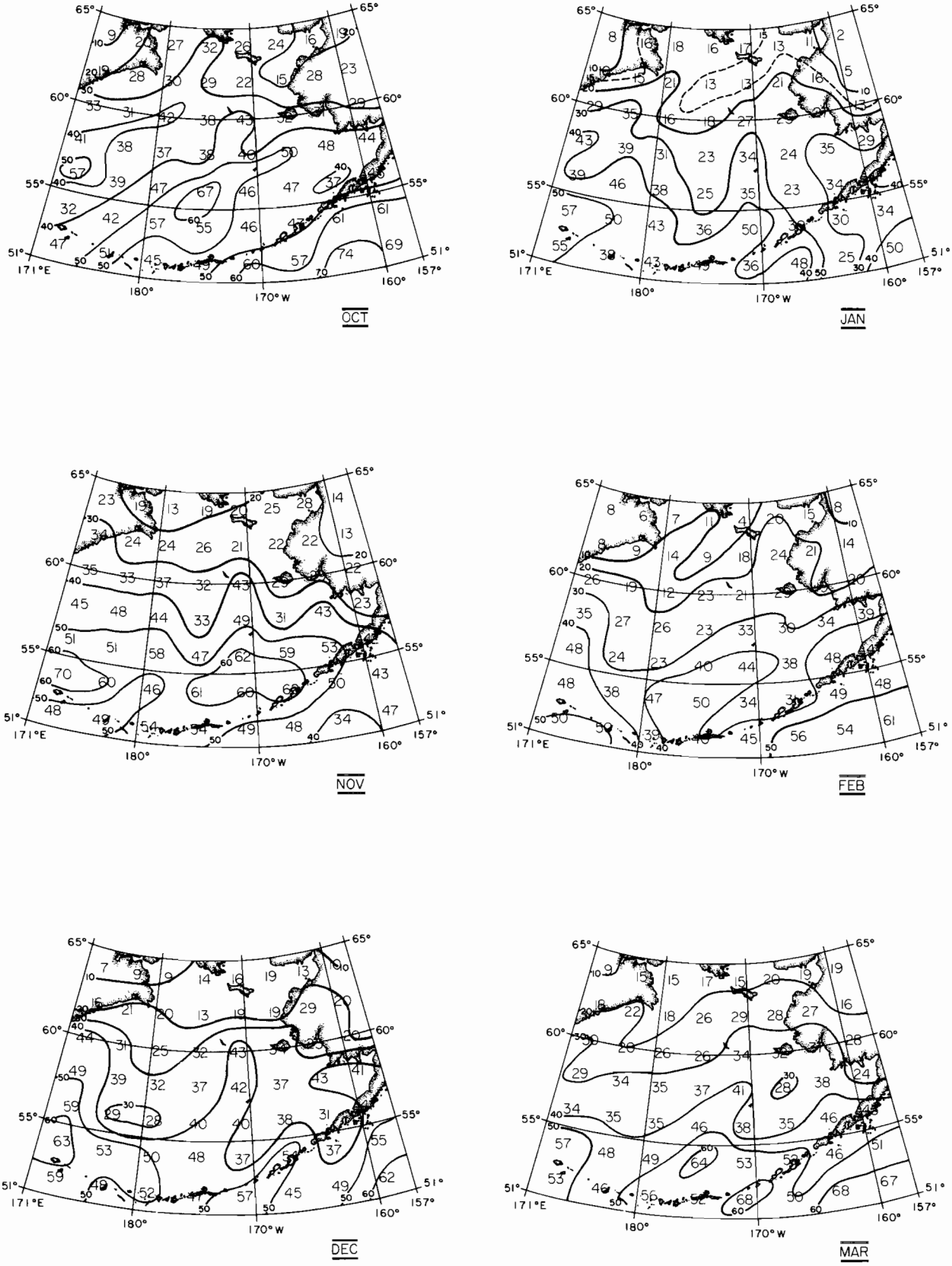

Figure 6.--Cyclone counts, using a 2°-latitude by 4°-longitude grid, for 23 years (1957/58 to 1979/80) summed by month (October-March).

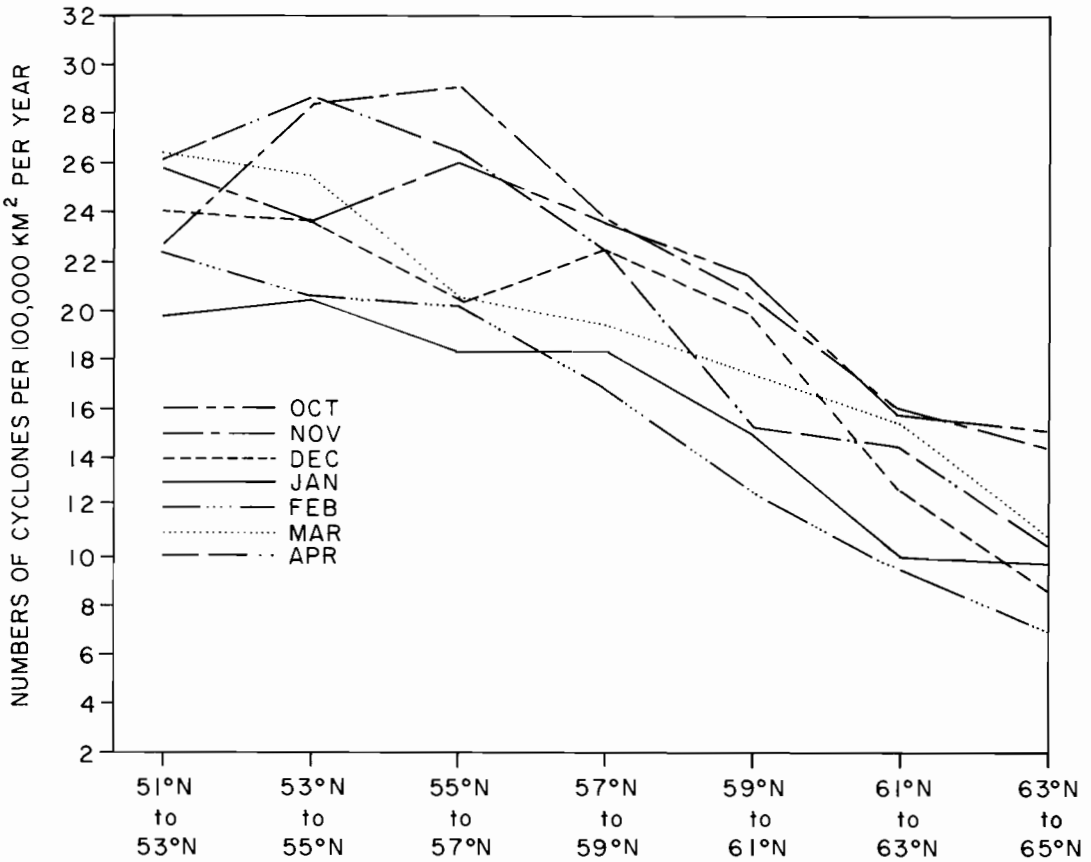

Figure 7.--Cyclone frequency between 160°W and 180°W as a function of month and latitude.

4.3 Relation to Sea Ice Extent

The average 5-mo storm pattern (October through February) is given in fig. 8. Storms pass zonally from west to east and decrease in number with increasing latitude. There is also a suggestion of a slight preference for tracks to follow either the Siberian or Alaskan coastline. The five heavy ice years (fig. 9) are characterized by a maximum of storm centers at 170°W, 51°N in the southeast Bering. Fewer storms penetrate north of 60°N than in an average year, although the tendency for secondary preferred tracks along either coast is still present. The light ice years (fig. 10) are characterized by a pronounced maximum of storm centers at 177°E, 54°N in the southwest Bering. The preferred track is shifted northward from south of the Aleutians to about 56°N. There is also a preference for storms in the western portion of the basin at 60°N. In general there are more storms throughout the basin than in an average winter. The maximum number of storms for both light and heavy ice years occur in the southern portion of the region beyond the limit of ice extent. The longitude of the maximum number of cyclones and preferred track are the primary differences between light and heavy ice years. Figure 11 shows the storm pattern for the years of greatest minus least ice extent, which dramatically indicates the influence of the east-west storm track preference.

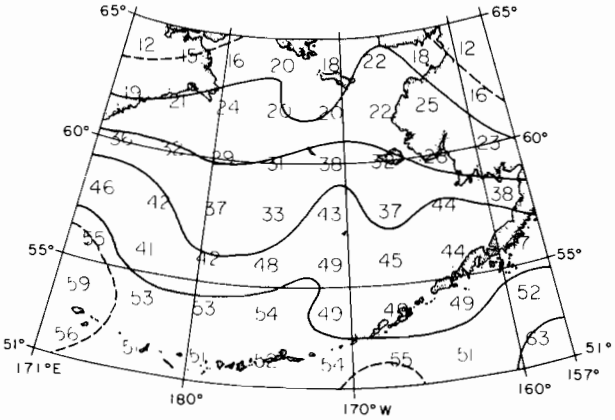

Figure 8.--Average number of cyclones, using a 2°-latitude by 4°-latitude grid, for 5 months (October-February) scaled over 5 years. Dashed lines are half-interval contours.

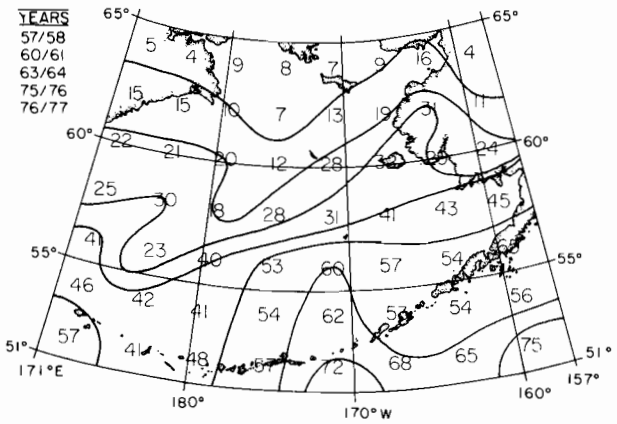

Figure 9.--Storm track counts for October-February of the five heaviest ice years.

Of the five years identified in table 1 as heavy ice extent years, 1976/77 was the least significant of the choices. There were other years that were statistically similar, such as 1971/72, and a reanalysis of the cyclone center pattern with 1971/72 instead of 1976/77 gave results similar to those in fig. 9. Likewise, of the five years identified in table 1 as light ice extent years, 1977/78 was the least significant of the choices. Reanalysis of the storm center pattern with 1968/69 substituted for 1977/78 gave results similar to those in fig. 10.

The first empirical orthogonal function (fig. 12) is qualitatively similar to the difference pattern for maximum-minus-minimum ice years

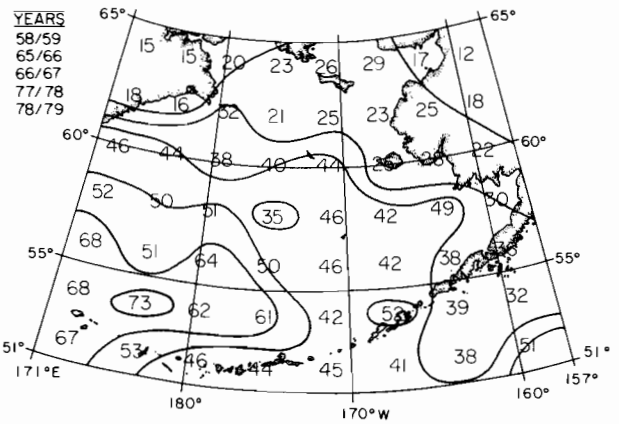

Figure 10.--Storm track counts for October-February of the five lightest ice years.

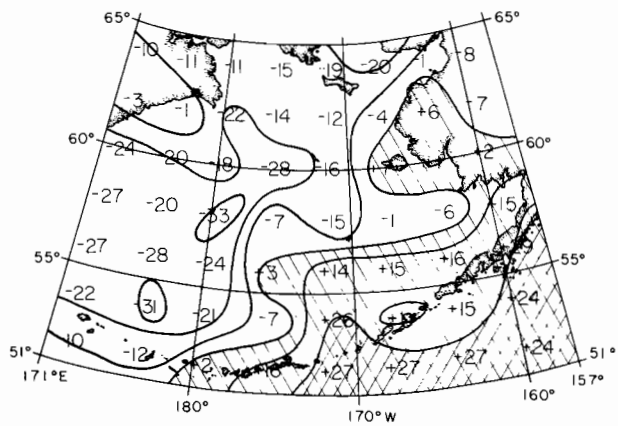

Figure 11.--Cyclone counts for five years of maximum ice extent minus cyclone counts for five years of minimum ice extent.

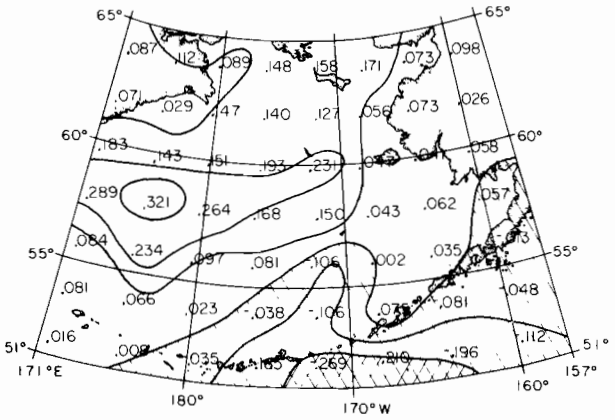

Figure 12.--First empirical orthogonal function of cyclone counts October-February for 1957-1980.

(fig. 11). Results presented in figs. 11 and 12 suggest that the number of storms penetrating the northern Bering Sea are correlated with western storm tracks. This is in fact the case; the correlation of index 1 with index 2 (negative implies western tracks) is r = -0.43 for the 22 years of record. Ice year 1961/62 was excluded from the correlation because the ice extent is uncertain. The ice extent correlated with index 1 is r = 0.71, and the correlation with index 2 is r = -0.30 (table 2). The correlations of both index 1 and the first EOF with the ice extent are significant at the 95% level. This suggests that ice extent is a function primarily of storm track preference. Figure 13 plots index 1 and the maximum ice extent, each as a function of ice year.

Table 2.--Correlation of ice extent with three storm indices[1]

	Ice extent (km)	E-W (Index 1)	North of 59° (Index 2)	EOF (Index 3)
Mean	812.2	3.00	17.13	0.00
Standard deviation	114.5	39.82	5.60	0.958
Correlation with ice extent[2]		0.707	0.295	0.511

[1] Ice year 1961/62 is not included.
[2] A correlation of r > 0.423 is significant for the 5% critical point with 20 degrees of freedom.

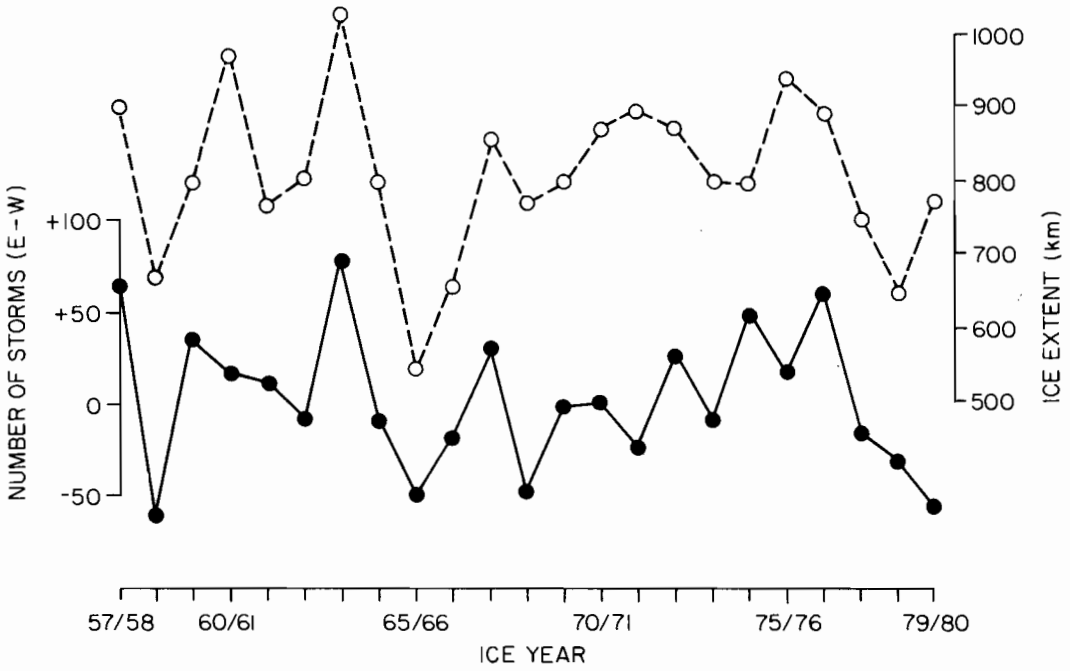

Figure 13.--Number of storms in the eastern sector minus number in the western sector (cyclone index 1) and ice extent, each as a function of year.

The correlation between index 2 and the normalized ice extent is negative, as expected, but the correlation is low. This indicates that there is a tendency for fewer storms in heavy ice years than in light ice years, although the correlation is not significant. The low correlation for index 2 is dramatized by the winter of 1963/64, the heaviest ice year in this record, which had an average number of storms over the northern and western sectors, but which showed an unusually large number of storms along the Alaska Peninsula.

5. PRESSURE CLIMATOLOGY

5.1 Methods

Five-day block-averaged sea level pressure (SLP) fields for the Northern Hemisphere were obtained on the Fleet Weather Facility's grid from the Joint Institute for the Study of the Atmosphere and the Ocean (JISAO, University of Washington, Seattle, WA 98195). The data set extended to 1946, but the pressure climatology analysis was started with the winter of 1954/55 to more closely parallel the analysis periods of the ice and storm track climatologies. Twenty-three years, October through February, were analyzed using METLIB, a program library for calculating and plotting marine boundary layer fields (Overland et al., 1980).

Averages for each month were formed over the 23 years to estimate the intraseasonal variation of the pressure fields; a composite winter average including all months (October-February) and all years (1954/55 to 1976/77) was made for comparison with subset composites for heavy and light ice years. Since the pressure data set did not include the light ice years 1977/78 and 1978/79, the next lightest years were identified in table 1 and substituted in the 5-yr averages. The heavy ice years were the same as for the storm track climatology.

5.2 Annual Cycle

Figure 14 shows the average SLP over 23 years (1954/55 to 1976/77) for each month (October-February). Each pattern suggests the same latitude for the paths of low-pressure systems as did the annual cycle calculated for the storm track climatology (fig. 6). The pressure data are much coarser, 381-km grid spacing, compared with about 222-km grid spacing for the storm track data, so the pressure plots are by necessity very smooth. October has a tendency for a low-pressure system to be centered over the eastern Alaska Peninsula and Kodiak Island. The sharpest curvature in the 1004-mb and 1008-mb contours occur at the same latitudes as the northern storm track for October in fig. 6. November's minimum pressure is through the southern Bering Sea at about 54°-55° latitude. This also parallels the maximum storm track path. December is similar except the minimum pressure has moved farther south; in January, it has moved farther south still. The 1004-mb contour on the January map closely follows the northwest-southeast trend of the 30-storm contour in the storm track map (fig. 6). February's map is similar to December. The 5-mo composite field is most similar to the November and December maps (fig. 15). The major features are the 1016-mb high-pressure area over Siberia, the relatively zonal isobars, and the <1004-mb trough paralleling the Aleutian Islands.

5.3 Relation to Sea Ice Extent

Figure 16 shows the average SLP pattern for the five heaviest ice years. This pattern looks very much like the average condition: a well-formed Aleutian low-pressure center, a strong high-pressure center over Siberia, and isobar lines oriented northeast-southwest in the optimum pattern for advection of ice on the conveyor belt. The anomaly pattern--heavy ice pattern minus average pattern (fig. 17)--has features similar to the average, but with a deeper low pressure. Although highly smoothed, the features mimic the storm track pattern closely.

Similarly, fig. 18 shows the average SLP pattern for the five lightest ice years. A minimum occurs in the pressure pattern over the southwest. Also, pressures seem higher over most of the pattern; this is supported by the plot of the anomaly pattern (fig. 19). The heavy and light ice year pressure anomalies have the same general shape but are opposite in sign, which supports strongly the concept of a hinge or oscillation in the pressure pattern along the northeast-southwest axis. In fact, the difference pattern between heavy and light years (fig. 20) shows a high degree of colinearity of the shapes.

In heavy ice years there is a tendency for storms to propagate zonally across the southern Bering, allowing for the establishment of high pressure north of the basin, or for the propagation of storms northward along the

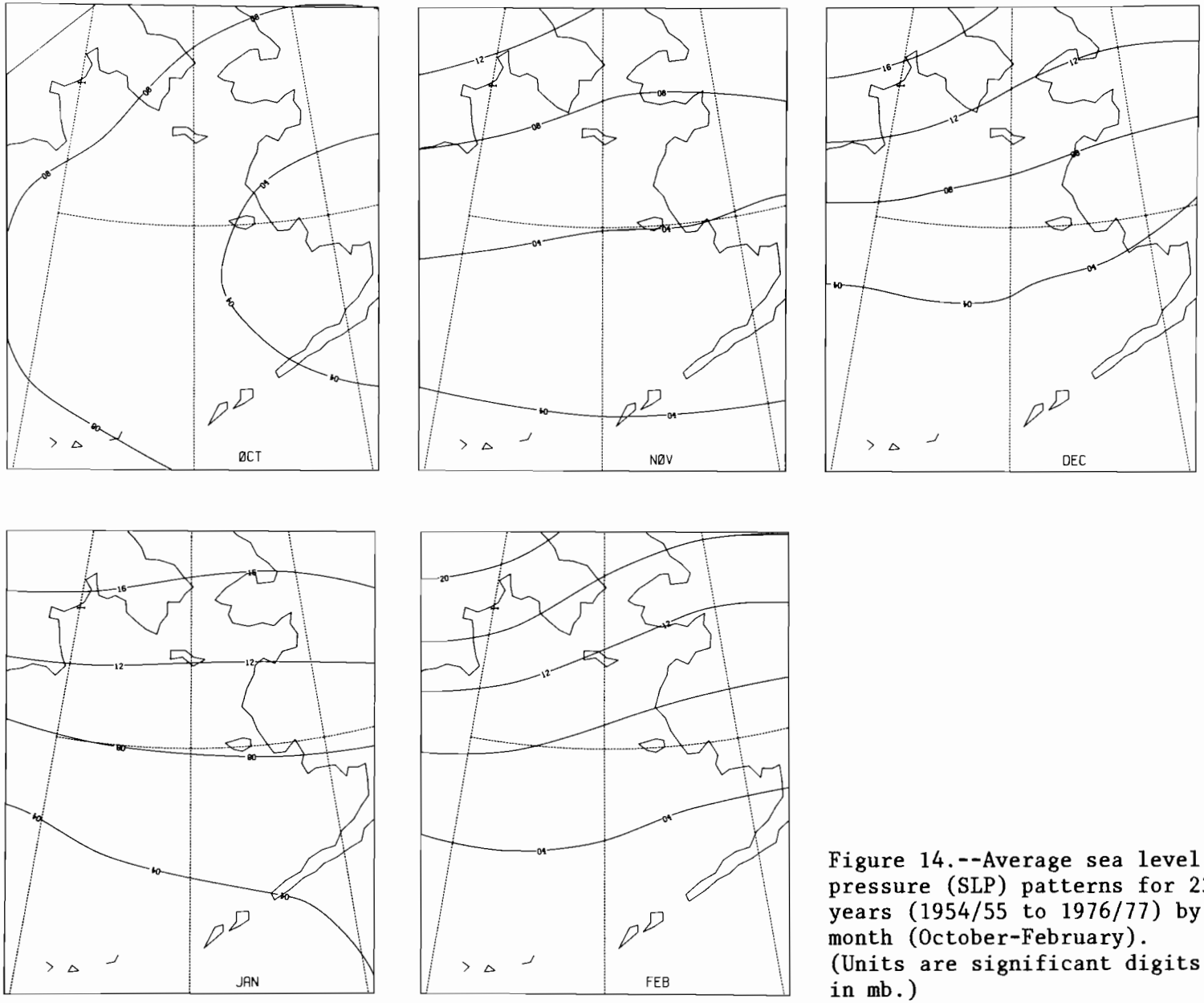

Figure 14.--Average sea level pressure (SLP) patterns for 23 years (1954/55 to 1976/77) by month (October-February). (Units are significant digits in mb.)

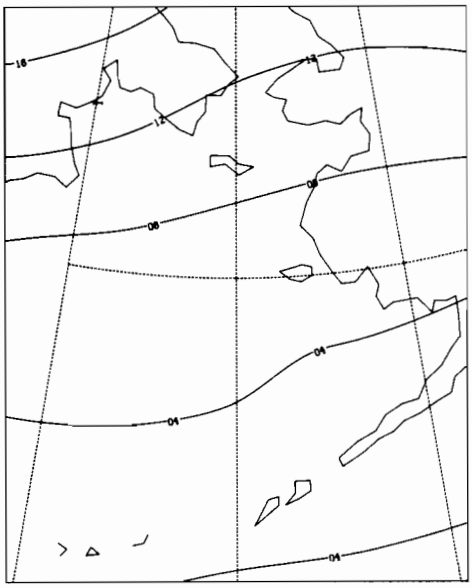

Figure 15.--Average winter (October-February) SLP pattern for 1954/55 to 1976/77. (Units are significant digits in mb.)

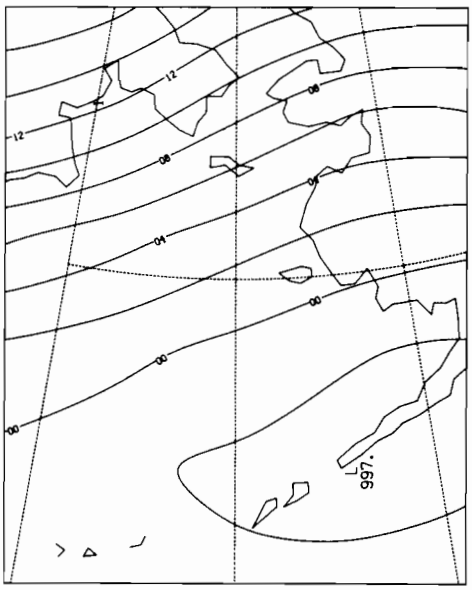

Figure 16.--Average winter (October-February) SLP pattern for five heaviest ice years. See fig. 9 for years. (Units are significant digits in mb.)

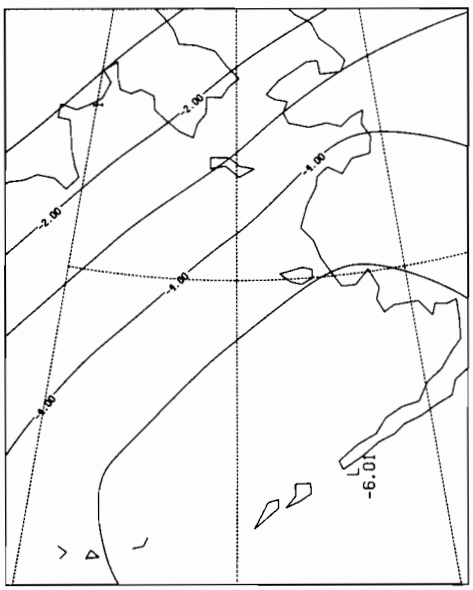

Figure 17.--Anomaly winter (October-February) SLP pattern; i.e., pattern for five heaviest ice years minus the average pattern. See fig. 9 for years. (Units are mb.)

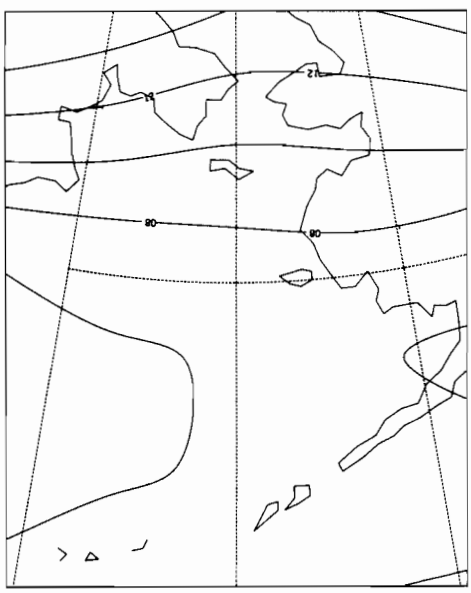

Figure 18.--Average winter (October-February) SLP pattern for five lightest ice years. See fig. 10 for years. (Units are significant digits in mb.)

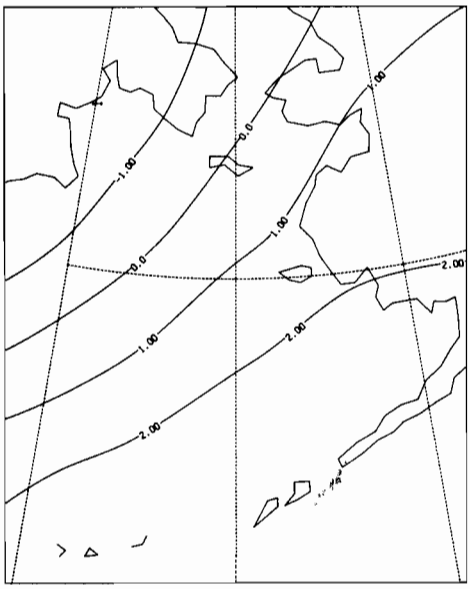

Figure 19.--Anomaly winter (October-February) SLP pattern; i.e., pattern for five lightest ice years minus the average pattern. See fig. 10 for years. (Units are mb.)

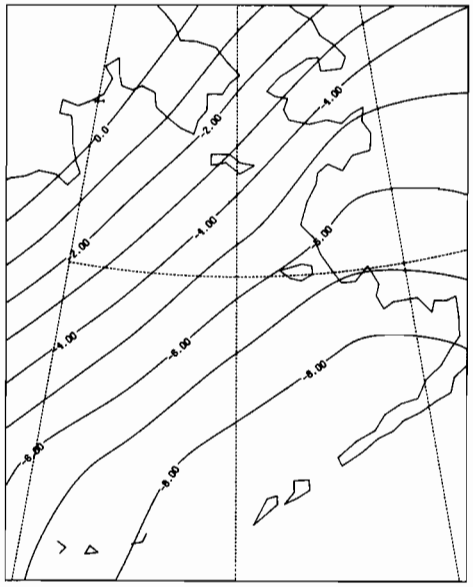

Figure 20.--Difference SLP pattern for the five heaviest minus the five lightest ice years. See figs. 9 and 10 for years. (Units are mb.)

Alaskan side of the Bering Sea. Both situations result in advection of cold, dry air from Alaska and the Arctic over the ice growth regions in the coastal polynyas, and both vigorously drive the ice southward. In light ice years there is a tendency for more storms and for the storms to propagate up the Siberian side. This exposes the ice to warm, moist air from the Pacific, drives the ice northward to the limits of the internal pack strength, and closes the polynya growth regions.

6. PRESSURE VARIANCE

6.1 Methods

The pressure data set described in sec. 5 was used for the following pressure variance calculations. The observed pressure, p, (in this case the 5-day-averaged pressure) can be written

$$p = \bar{p} + p'$$

where $\bar{p}$ is the mean pressure for the year and p' is the time-varying fluctuation in pressure. From the p' values, the pressure variance, $\overline{p'^2}$, can be calculated for individual years and averaged for all years, for the five heavy ice years, and for the five light ice years. Because these data are 5-day means, care should be taken in comparing these variance statistics with calculations from other pressure data sets. The pressure variances calculated in this study would be uniformly lower than variances calculated from synoptic data sets, but the trends would be the same on seasonal time scales.

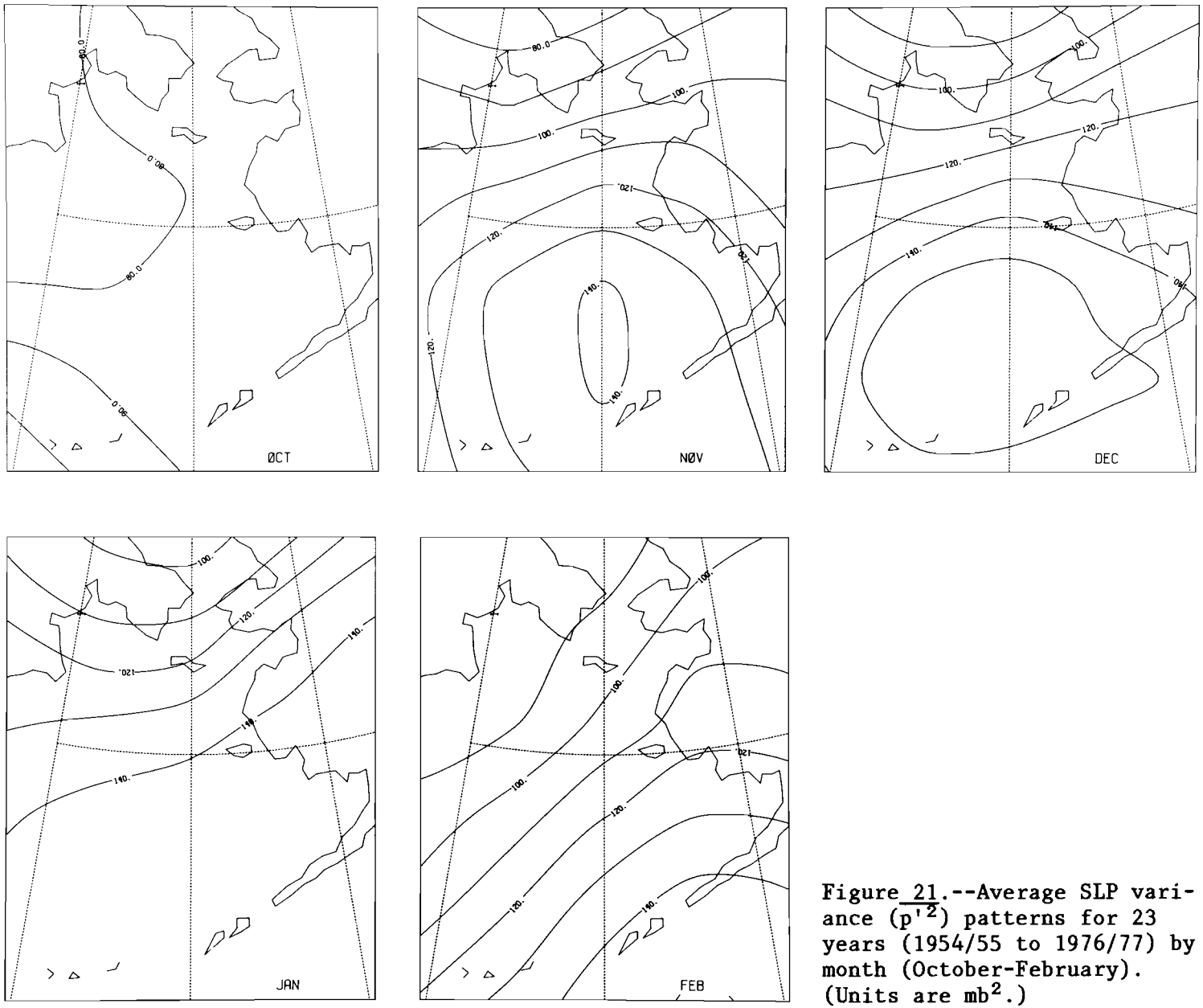

Figure 21.--Average SLP variance ($\overline{p'^2}$) patterns for 23 years (1954/55 to 1976/77) by month (October-February). (Units are mb^2.)

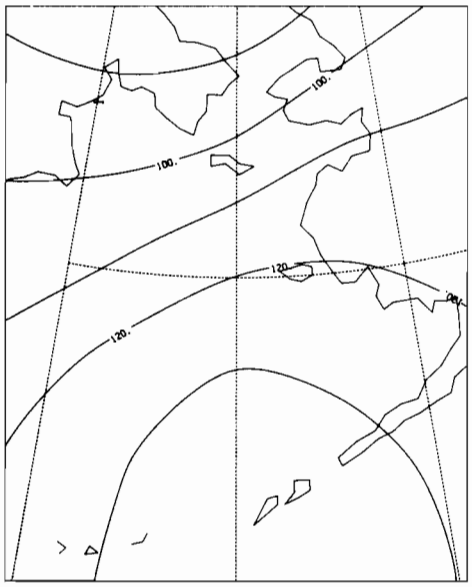

Figure 22.--Average winter (October-February) SLP variance ($\overline{p'^2}$) pattern for 23 years (1954/55 to 1976/77). (Units are mb^2.)

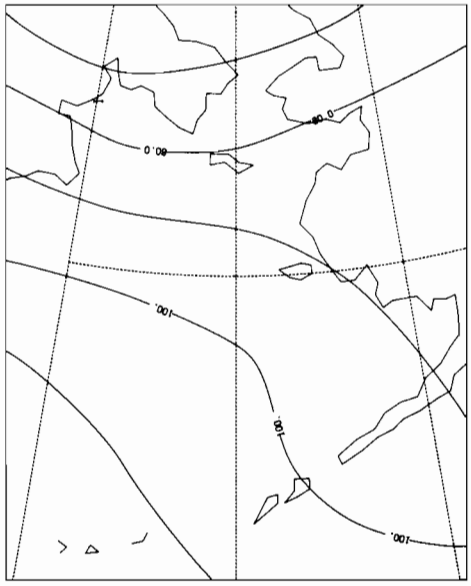

Figure 23.--Average winter (October-February) SLP variance ($\overline{p'^2}$) pattern for five heaviest ice years. See fig. 9 for years. (Units are mb^2.)

6.2 Annual Cycle

Figure 21 shows the average SLP variance over 23 years (1954/55 to 1976/77) for each month (October-February). October has the least organized variance pattern compared with other winter months. By contrast, November exhibits increased structure and has high variance concentrated in the south central Bering Sea (55°N and 170°W) and decreasing variance toward the north. The variance maximum is centered exactly over the storm count maximum in fig. 6. By December the pressure variance in the south has increased and broadened in range (fig. 21), a trend that continues through January. In February the variance of the pressure decreases and is focused southeast of the Aleutian Islands. These monthly trends follow the storm count maxima and mean pressure minima (fig. 14) closely. Thus, the region in the southern Bering Sea with the largest variations from the mean winter pressure (fig. 22) is the preferred storm track path. This corroborates the storm track statistics within the resolution of the pressure fields.

6.3 Relation to Sea Ice Extent

Figure 23 shows the pressure variance averaged for five heavy ice years. The 23-yr average pattern (fig. 22) has a maximum over the central Aleutians, and a general decrease in variance toward the north suggesting that few storms move northward. The heavy ice year variance is reduced from the average pattern, and the maximum is shifted to the southwest. This may be seen more easily in the heavy ice year anomaly pattern (fig. 24), which indicates the distinct east-west change. This would be consistent with the idea that lows are quasi-stationary over Kodiak Island and the Alaskan Peninsula during heavy ice years.

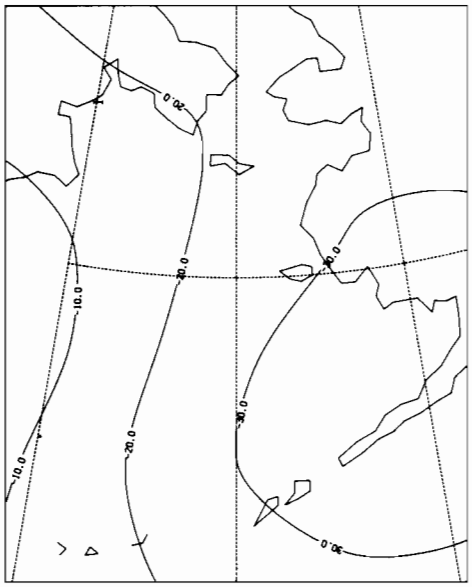

Figure 24.--Anomaly SLP variance ($\overline{p'^2}$) pattern; i.e., variance pattern ($\overline{p'^2}$) for five heaviest ice years minus average variance pattern (October-February). See fig. 9 for years. (Units are mb^2.)

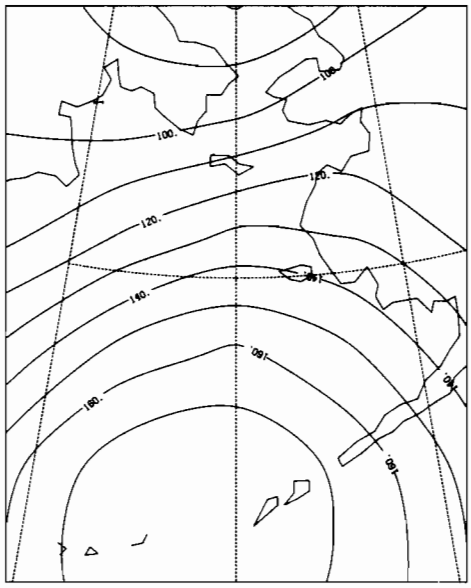

Figure 25.--Average winter (October-February) SLP variance ($\overline{p'^2}$) pattern for five lightest ice years. See fig. 10 for years. (Units are mb^2.)

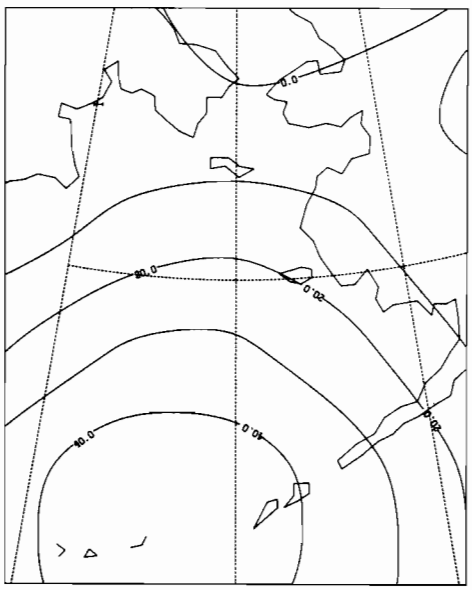

Figure 26.--Anomaly SLP variance ($\overline{p'^2}$) pattern; i.e., variance pattern ($\overline{p'^2}$) for five lightest ice years minus average variance pattern (October-February). See fig. 10 for years. (Units are mb^2.)

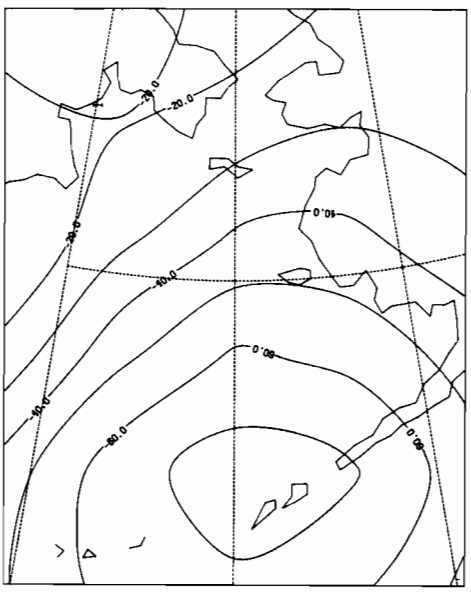

Figure 27.--Difference SLP variance ($\overline{p'^2}$) pattern for five heaviest minus the five lightest ice years. See figs. 9 and 10 for years. (Units are mb^2.)

The light ice year variance is increased everywhere over the average (fig. 25) and has higher gradients than either the 23-yr-averaged or heavy ice year patterns. This is most noticeable in the light ice year anomaly pattern (fig. 26), which indicates the marked increase of storm activity in the southwestern Bering Sea in contrast to the average pattern.

The difference pattern between heavy and light ice years (fig. 27) emphasizes the distinct character of the two different types of ice years. The heavy ice years have less variance everywhere than the light years. In addition, light ice years are characterized by many storms penetrating the region, particularly along the western part of the basin; heavy ice years are characterized by fewer storms entering the region and by a tendency for low-pressure centers to be quasi-stationary over the western Gulf of Alaska and southeastern Bering Sea.

7. SUMMARY AND CONCLUSIONS

On the basis of 23 years of data, a storm track climatology has been developed for the Bering Sea in the winter season, October through February, using a 2°-latitude by 4°-longitude grid. The seasonal trend shows a decreased number of storms in January and February. There is a decrease in storms with increasing latitude in all months. There is a tendency for two primary storm tracks: one parallel to the Aleutian Island chain and one curving northward into the northern Bering Sea. The predominance of the northern track relative to the southern track is most significant in January.

Maximum ice extents in the Bering Sea are computed for ice years 1955/56 to 1979/80. The relative accuracy when compared with satellite observations for 1968/69 to 1979/80 is about ±50 km. The relative accuracy is about ±100 km when compared with direct observations from ships or ice reconnaissance flights before 1968/69, except for 1961/62, which had no direct observations published in the standard literature. The distribution of ice extent is skewed toward heavy ice years.

The difference in the storm track patterns for the five heaviest and five lightest ice years shows a major shift in storm track. In light ice years the cyclones tend to propagate up the western side of the Bering Sea. The high correlation between east-west preference for storm track and ice extent suggests that a sufficient number of storms were represented each winter for the intensity variations to average out over any given winter.

To test the veracity of the storm track climatology, mean sea level pressure and pressure variance climatologies were constructed from 5-day-averaged SLP fields. The mean pressure for a heavy ice year is as much as 6 mb lower over the eastern Aleutian Islands and western Gulf of Alaska than for an average winter; the mean pressure for a light ice year is greater than the average, by about 2 mb, over the southeastern Bering Sea and western Gulf of Alaska. The pressure variances showed lower-than-normal values in heavy ice years, especially in the east, and higher-than-normal values in light ice years, especially in the west. These results are consonant with more transient storm activity in light ice years and less activity in heavy ones.

Considering the possibility for errors in the various indices, the high correlation between ice extent and storm track preference indicates that meteorological steering of cyclones, determined externally to the Bering Sea, is the primary factor causing interannual variability of sea ice extent. Further studies comparing patterns of upper-level flow during heavy and light ice years and examining the maintenance of significant anomalies in these patterns could establish a relation between large-scale atmospheric features and regional ice extent.

8. ACKNOWLEDGMENTS

This report is a contribution to the Marine Services project at the Pacific Marine Environmental Laboratory. It was supported in part by the Bureau of Land Management through an interagency agreement with the National Oceanic and Atmospheric Administration under which a multiyear program is being conducted to respond to the need for petroleum development on the Alaskan continental shelf. The program is managed by the Outer Continental Shelf Environmental Assessment Program (OCSEAP). Programing assistance was provided by Judith Gray.

9. REFERENCES

Barry, R. G., 1977. Study of climatic effects on fast ice extent and its seasonal decay along the Beaufort-Chuckchi coasts. In *Environmental Assessment of the Alaskan Continental Shelf: Vol. XIV, Transport,* NOAA Environmental Research Laboratories, Boulder, Colo., 574-743.

Barry, R. G., and A. H. Perry, 1973. *Synoptic Climatology, Methods and Applications*. Methuen, London, 553 pp.

Blackmon, M. L., J. M. Wallace, N. Lau, and S. L. Mullen, 1977. An observational study of the Northern Hemisphere wintertime circulation. *J. Atmos. Sci.* 34:1040-1053.

Blasing, T. J. and H. C. Fritts, 1976. Reconstructing past climatic anomalies in North Pacific and western North America from tree-ring data. *Quarternary Res.* 6:563-579.

Campbell, W. J., P. Gloersen, and R. O. Ranseier, 1974. Synoptic ice dynamics and atmospheric circulation during the Bering Sea Experiment. *Results of the U.S. Contribution to the Joint U.S./U.S.S.R. Bering Sea Experiment,* Rep. X-910-74-141, NASA Goddard Space Flight Center, Greenbelt, Md., 1-30.

Crane, R. G., 1978. Seasonal variations of sea ice extent in the Davis Strait-Labrador Sea area and relationships with synoptic-scale atmospheric circulation. *Arctic* 31:434-447.

Dunbar, R. G., 1967. The monthly and extreme limits of ice in the Bering Sea. *Physics of Snow and Ice,* Vol. 1, Institute of Low Temperature Science, University of Hokkaido, Hokkaido, Japan, 687-703.

Fay, F. H., 1974. The role of ice in the ecology of marine mammals of the Bering Sea. In *Oceanography of the Bering Sea*, D. W. Hood and E. J. Kelley (eds.), Institute of Marine Sciences, University of Alaska, Fairbanks, 383-399.

Hayden, B. P., 1981. Cyclone occurrence mapping: equal area or raw frequencies. *Mon. Weather Rev.* 109:168-172.

Johnson, C. M., 1980. Wintertime Arctic sea ice extremes and the simultaneous atmospheric circulation. *Mon. Weather Rev.* 108:1782-1791.

Kinder, T. H., and J. D. Schumacher, 1981a. Hydrographic structure over the Continental Shelf of the southeastern Bering Sea. In *The Eastern Bering Sea Shelf: Oceanography and Resources*, Vol. 1, D. W. Hood and J. A. Calder (eds.), University of Washington Press, Seattle (available from Government Printing Office, 796-495, Washington, D.C.), 31-52.

Kinder, T. H., and J. D. Schumacher, 1981b. Circulation over the Continental Shelf of the southestern Bering Sea. In *The Eastern Bering Sea Shelf: Oceanography and Resources*, Vol. 1, D. W. Hood and J. A. Calder (eds.), University of Washington Press, Seattle (available from Government Printing Office, 796-495, Washington, D.C.), 53-75.

Klein, W. H., 1957. *Principal tracks and mean frequencies of cyclones and anticyclones in the northern hemisphere*. Res. Paper No. 40, U.S. Weather Bureau, Washington, D.C., 60 pp.

McNutt, L., 1981a. *Ice conditions in the Eastern Bering Sea from NOAA and LANDSAT imagery: winter conditions 1974, 1976, 1977, 1979*. NOAA Tech. Memo. ERL PMEL-24, NOAA Environmental Research Laboratories, Boulder, Colo., 179 pp.

McNutt, S. L., 1981b. Remote sensing analysis of the ice growth and distribution in the eastern Bering Sea. In *The Eastern Bering Sea Shelf: Oceanography and Resources*, Vol. 1., D. W. Hood and J. A. Calder (eds.), University of Washington Press, Seattle (available from Government Printing Office, 796-495, Washington, D.C.), 141-166.

Muench, R. D., and K. Ahlnäs, 1976. Ice movement and distribution in the Bering Sea from March to June 1974. *J. Geophys. Res.* 81:4467-4476.

Niebauer, H. J., 1980. Sea ice and temperature variability in the eastern Bering Sea and the relation to atmospheric fluctuations. *J. Geophys. Res.* 85:7507-7515.

Overland, J. E., and T. R. Hiester, 1980. Development of a synoptic climatology for the northeast Gulf of Alaska. *J. Appl. Meteorol.* 19:1-14.

Overland, J. E., and R. W. Preisendorfer, 1982. A significance test for principal components applied to a storm track climatology. *Mon. Weather Rev.* 110:1-4.

Overland, J. E., R. A. Brown, and C. D. Mobley, 1980. *METLIB--a program library for calculating and plotting marine boundary layer wind fields*. NOAA Tech. Memo. ERL PMEL-20, NOAA Environmental Research Laboratories, Boulder, Colo., 82 pp.

Pease, C. H., 1980. Eastern Bering Sea ice processes. *Mon. Weather Rev.* 108:2015-2023.

Pease, C. H., and R. D. Muench, 1981. Sea ice study cruise observes gale effects. *Coast. Oceanogr. Climatol. News* 3(4):43-45.

Petterssen, S., 1956. *Weather Analysis and Forecasting.* Vol. 1, McGraw-Hill, New York, 442 pp.

Preisendorfer, R. W., and T. P. Barnett, 1977. Significance tests for empirical orthogonal functions. *Proceedings of Fifth Conference on Probability and Statistics,* Nov. 15-18, 1977, Las Vegas, Nevada, American Meteorological Society, Boston, Mass., 169-172.

Putnins, P., 1966. *Studies on the meteorology of Alaska: the sequence of baric pressure patterns over Alaska.* First Interim Report, ESSA Environmental Data Service, Silver Spring, Md., 57 pp.

Rogers, J. C., 1978. Meteorological factors affecting interannual variability of summertime ice extent in the Beaufort Sea. *Mon. Weather Rev.* 106:890-897.

Rogers, J. C., 1981. The North Pacific oscillation. *J. Climatol.* 1:39-57.

Salo, S. A., C. H. Pease, and R. W. Lindsay, 1980. *Physical environment of the Eastern Bering Sea, March 1979.* NOAA Tech. Memo. ERL PMEL-21, NOAA Environmental Research Laboratories, Boulder, Colo., 119 pp.

Schell, I. I., 1964. Interrelations of ice off northern Japan and the weather. *J. Meteorol. Soc. Japan* 42:174-185.

Schwerdtferger, W., and S. Kachelhoffer, 1973. The frequency of cyclonic vortices over the southern ocean in relation to the extension of the pack ice belt. *Antarct. J. U. S.* 8:234.

Suckling, P. W., and J. E. Hay, 1978. On the use of synoptic weather map typing to define solar radiation regimes. *Mon. Weather Rev.* 106:1521-1531.

Wadhams, P., 1981. The ice cover in the Greenland and Norwegian Seas. *Rev. Geophys. Space Phys.* 19:345-393.

Walker, G. T., and E. W. Bliss, 1932. World Weather V. *Mem. Roy. Meteorol. Soc.* 4:53-84.

Walsh, J. E., and C. M. Johnson, 1979a. An analysis of Arctic sea ice fluctuations, 1953 to 1977. *J. Phys. Oceanogr.* 9:580-591.

Walsh, J. E., and C. M. Johnson, 1979b. Interannual atmospheric variability and associated fluctuations in Arctic sea ice extent. *J. Geophys. Res.* 84:6915-6928.

Walter, B. A., 1980. Wintertime observations of roll clouds over the Bering Sea. *Mon. Weather Rev.* 108:2024-2031.

Webster, B. D., 1979. *Ice edge probabilities for the Eastern Bering Sea.* NOAA Tech. Memo. NWS AR-26, NOAA National Weather Service, Alaska Region, Anchorage, Alaska, 20 pp.

White, W. B., and N. E. Clark, 1975. On the development of blocking ridge activity over the central north Pacific. *J. Atmos. Sci.* 32:489-502.

Wiese, W., 1924. Polareis and atmosphärische Schwankungen. *Geogr. Ann.* 6:273-299.

WMO (World Meteorological Organization), 1970. ***WMO Sea-Ice Nomenclature.*** WMO/OMM/BMO no. 259, Tech. Publ. 145, Geneva, Switzerland, 147 pp.

Zishka, K. M., and P. J. Smith, 1980. The climatology of cyclones and anticyclones over North America and surrounding ocean environs for January and July, 1950 to 1977. *Mon. Weather Rev.* 108:387-401.

Glossary of WMO Sea Ice Terms

The following ice nomenclature is abridged from a list adopted and published by the World Meteorological Organization (WMO, 1970).

Brash ice: Accumulations of *floating ice* made up of fragments not more than 2 m across, the wreckage of other forms of ice.

Compacting: Pieces of *floating ice* are said to be compacting when they are subjected to a converging motion, which increases ice *concentration* and/or produces stresses which may result in ice deformation.

Concentration: The ratio in tenths of the sea surface actually covered by ice to the total area of sea surface, both ice-covered and *ice-free*, at a specific location or over a defined area.

Diverging: *Ice fields or floes* in an area are subjected to diverging or dispersive motion, thus reducing ice *concentration* and/or relieving stresses in the ice.

Fast ice: *Sea ice* which forms and remains fast along the coast, where it is attached to the shore. Vertical fluctuations may be observed during changes of sea-level. Fast ice may be formed *in situ* from sea water or by freezing of *pack ice* of any age to the shore, and it may extend a few metres or several hundred kilmetres from the coast.

Finger rafting: Type of rafting whereby interlocking thrusts are formed, each floe thrusting "fingers" alternately over and under the other. Common in *nilas* and *gray ice*.

Firn: Old snow which has recrystallized into a dense material. Unlike snow, the particles are to some extent joined together; but, unlike ice, the air spaces in it still connect with each other.

First-year ice: *Sea ice* of not more than one winter's growth, developing from *young ice*; thickness 30 cm to 2 m. May be subdivided into *thin first-year ice*/white ice, *medium first-year ice* and *thick first-year ice*.

Flaw: A narrow separation zone between *pack ice* and *fast ice*, where the pieces of ice are in chaotic state; it forms when pack ice shears under the effect of a strong wind or current along the *fast ice boundary*.

Floe: Any relatively flat piece of *sea ice* 20 m or more across. Floes are subdivided according to horizontal extent as follows:
Giant: Over 10 km across.
Vast: 2-10 km across.
Big: 500-2,000 m across.
Medium: 100-500 m across.
Small: 20-100 m across.

Flooded ice: *Sea ice* which has been flooded by meltwater or river water and is heavily loaded by water and wet snow.

Ice boundary: The demarcation at any given time between *fast ice* and *pack ice* or between areas of *pack ice* of different *concentrations*.

Ice breccia: Ice pieces of different age frozen together.

Lead: Any *fracture* or passage-way through *sea ice* which is navigable by surface vessels. [Author's note: More typically taken to mean long linear opening of water between floes or groups of floes of 1 m to 100 m across and 100 m to a few kilometers long.]

New ice: A general term for recently formed ice which includes *frazil ice, grease ice, slush,* and *shuga*. These types of ice are composed of ice crystals which are only weakly frozen together (if at all) and have a definite form only while they are afloat.

Nilas: A thin elastic crust of ice, easily bending on waves and swell and under pressure, thrusting in a pattern of interlocking "fingers" *(finger rafting)*. Has a matt surface and is up to 10 cm in thickness. May be subdivided into *dark nilas* and *light nilas*.

Open water: A large area of freely navigable water in which *sea ice* is present in *concentrations* of less than 1/10 (1/8). When there is no sea ice present, the area should be termed *ice-free*.

Pack ice: Term used in a wide sense to include any areas of sea ice, other than *fast ice,* no matter what form it takes or how it is disposed.

Polynya: Any non-linear shaped opening enclosed in ice. Polynya may contain *brash ice* and/or be covered with *new ice, nilas* or *young ice*. Sometimes a polynya is limited on one side by the coast and is called a *shore polynya* or by *fast ice* and is called a *flaw polynya*. If it recurs in the same position every year, it is called a *recurring polynya*.

Rafting: Pressure processes whereby one piece of ice overrides another. Most common in *new* and *young ice*.

Ridging: The pressure process by which *sea ice* is forced into *ridges*.

Sastrugi: Sharp irregular ridges formed on a snow surface by wind erosion and deposition.

Sea ice: Any form of ice found at sea which has originated from the freezing of sea water.

Shearing: An area of *pack ice* is subject to shear when the ice motion varies significantly in the direction normal to the motion, subjecting the ice to rotational forces. These forces may result in phenomena similar to a *flaw*.

Slush: Snow which is saturated and mixed with water on land or ice surfaces, or as a viscous floating mass in water after a heavy snowfall.

Snowdrift: An accumulation of wind-blown snow deposited in the lee of obstructions or heaped by wind eddies.

Young ice: Ice in the transition stage between *nilas* and *first-year ice,* 10-30 cm in thickness. May be subdivided into *gray ice* and *gray-white ice*.

☆ U.S. GOVERNMENT PRINTING OFFICE: 1982—576-001/1231 REGION No. 8